JCTC Journal of Chemical Theory and Computation

Article

pubs.acs.org/JCTC

Assessment of DFT Methods for Computing Activation Energies of Mo/W-Mediated Reactions

Lianrui Hu and Hui Chen*

Beijing National Laboratory for Molecular Sciences (BNLMS), CAS Key Laboratory of Photochemistry, Institute of Chemistry, Chinese Academy of Sciences, Beijing 100190, China

Supporting Information

ABSTRACT: Using high level ab initio coupled cluster calculations as reference, the performances of 15 commonly used density functionals (DFs) on activation energy calculations for typical Mo/W-mediated reactions have been systematically assessed for the first time in this work. The selected representative Mo/W-mediated reactions cover a wide range from enzymatic reactions to organometallic reactions, which include Mo-catalyzed aldehyde oxidation (aldehyde oxidoreductase), Mo-catalyzed dimethyl sulfoxide (DMSO) reduction (DMSO reductase), W-catalyzed acetylene hydration (acetylene hydratase), Mo/W-mediated olefin metathesis, Mo/W-mediated olefin epoxidation, W-mediated alkyne metathesis, and W-mediated C−H bond activation. Covering both Mo- and W-mediated reactions, four DFs of B2GP-PLYP, M06, B2-PLYP, and B3LYP are uniformly recommended with and without DFT empirical dispersion correction. Among these four DFs, B3LYP is notably improved in performance by DFT empirical dispersion correction. In addition to the absolute value of calculation error, if the trend of DFT results is also a consideration, B2GP-PLYP, B2-PLYP, and M06 keep better performance than other functionals tested and constitute our final recommendation of DFs for both Mo- and W-mediated reactions.

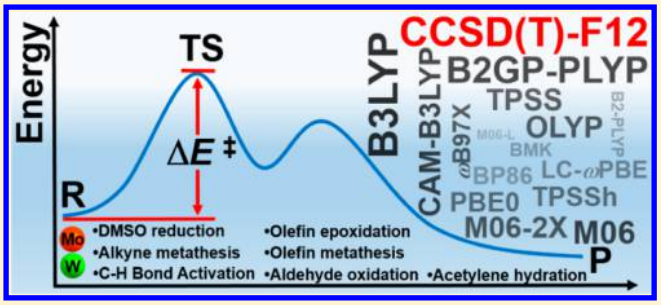

1. INTRODUCTION

Molybdenum (Mo) and tungsten (W) are two early 4d and 5d transition metals in group 6, which often exhibit similar reactivities in chemical reactions. In natural metalloenzymes, to our best knowledge, molybdenum/tungsten are the only known 4d/5d transition metals that act as a key cofactor in the active site. With this unique feature and their wide occurrence in transition metal catalysis and organometallic chemistry, Mo and W play essential roles in both biochemistry and organic chemistry.

Mononuclear molybdenum-containing enzymes constitute a large amount of significant enzymes in diverse organisms,[1−10] which can be categorized into different families by the cofactor coordinated to the metal center and the structure homology of the active site: xanthine oxidase, sulfite oxidase, and dimethyl sulfoxide (DMSO) reductase.[1,4,10] Aldehyde oxidoreductase (AOR) is one of the most important members of the xanthine oxidase, catalyzing the oxidation of aldehydes to corresponding acids.[11] The DMSO reductase family is the largest and most diverse group of mononuclear molybdenum enzymes. DMSO reductase catalyzes the oxygen-atom transfer from DMSO to the Mo^{IV} active site, yielding dimethyl sulfide (DMS) and Mo^{VI}.[1] In contrast to the diversity of molybdenum-containing enzymes, three families of enzymes have been discovered to be tungsten-dependent, namely, aldehyde oxidoreductase, formate dehydrogenase, and acetylene hydratase (AH).[3,4,8,12] Unlike aldehyde oxidoreductase and formate dehydrogenase involving oxidative process, AH catalyzes the nonredox hydration of acetylene in the anaerobic unsaturated hydrocarbon metabolism.[12,13]

Molybdenum and tungsten are also two of the most widely used early transition metals in organic and organometallic chemistry,[14−22] and many important organic reactions are mediated by Mo or W, such as alkene metathesis,[15,16,21,23−25] alkyne metathesis,[14,17,26−31] olefin epoxidation,[19,22,32−36] and C−H activation.[20,37−41] Molybdenum and ruthenium are the most frequently used transition metals to catalyze alkene metathesis. In contrast to alkene metathesis, for a very long time, the analogous alkyne metathesis is relatively less developed. Given the recent advances in the development of new alkyne metathesis catalysts,[14,29,42,43] several catalytic systems have been used so far for alkyne metathesis. Tungsten-based catalyst $(RO)_3W{\equiv}CR'$, the well-defined and now widely used tungsten alkylidyne complex, was one of the major breakthroughs in rational catalyst design for alkyne metathesis.[44−47] Due to the fact that ethylene oxide is an important chemical raw material, marvelous exploration efforts have focused on the epoxidation of olefins promoted by Mo/W.[19,22,32−36,48] As early as 20 years ago, BASF had reported and patented a promising method based on the stoichiometric epoxidation with a biphasic catalytic system of Mimoun-type diperoxomolybdenum

Received: April 21, 2015
Published: August 20, 2015

DOI: 10.1021/acs.jctc.5b00373
J. Chem. Theory Comput. 2015, 11, 4601−4614

complexes $[MoO(O_2)_2(OPR_3)]$ (R = NMe_2).[49−51] As an alternative promising strategy in organic synthetic methodology, recently C−H activation has attracted extensive research interests in organic and organometallic chemistry.[52−55] Notably tungsten-containing complex had been found to be capable of activating an inert sp^3 C−H bond of alkanes nearly 20 years ago.[20,56]

As collected in Scheme 1, the preceding typical chemical and biochemical reactions mediated by molybdenum and tungsten

Scheme 1. Mo/W-Mediated Reactions Studied in This Work

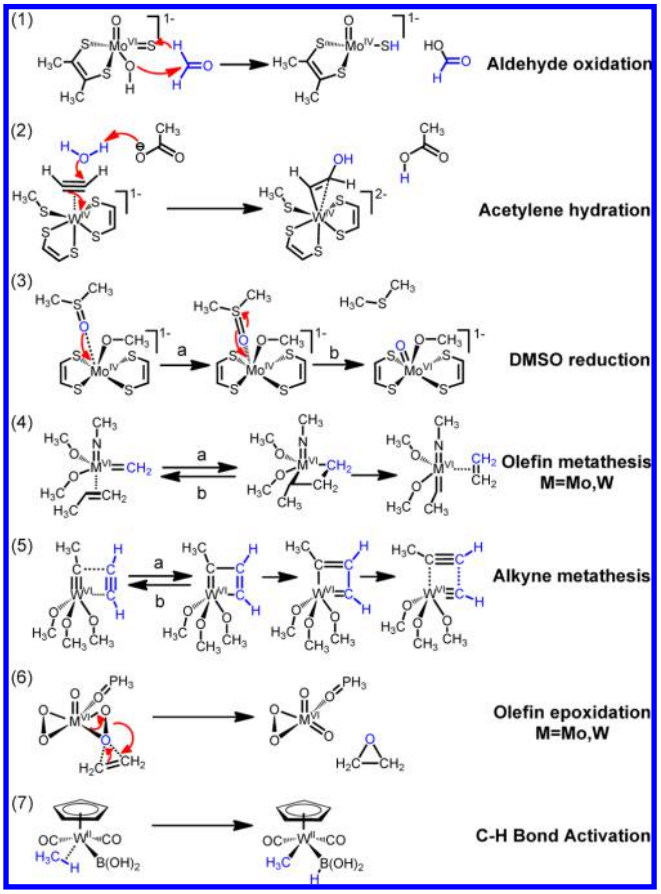

are of wide diversity. They cover Mo-mediated reactions, including formaldehyde oxidation catalyzed by AOR, DMSO reduction catalyzed by DMSO reductase, olefin metathesis, and olefin epoxidation, as well as W-mediated reactions, including acetylene hydration catalyzed by AH, olefin metathesis, alkyne metathesis, olefin epoxidation, and C−H bond activation. Their mechanisms have also been widely studied both experimentally and theoretically,[34,37,50,57−95] which enables us to focus only on crucial steps in reactions, such as the rate-limiting step or the step with relatively high activation energy, as depicted in Scheme 1.

In the past two decades, the development of computational chemistry, especially density-functional theory (DFT) methods, has contributed a lot to clarifying mechanisms of transition metal-mediated reactions. By locating the crucial points along the reaction pathway, such as minima and transition states, DFT methods have enabled one to get a great deal of details about reaction mechanism,[96−107] as evidenced also by the Mo- and W-mediated reaction mechanisms shown in Scheme 1. However, since different approximate density functionals (DFs) often show quite diverse performance for the same transition-metal-containing systems, many calibration studies have been done for the sake of choosing a more appropriate functional in barrier calculations.[84,108−134] High level ab initio calculations are often taken as reference for DFT calibration. For closed-shell systems without serious multiconfigurational character, such as many of ones containing 4d and 5d transition metals, CCSD(T) (the coupled cluster method with single and double excitations and a perturbative treatment of triple excitations),[135,136] which is a "gold standard" in modern quantum chemistry, is often a method of choice.

Particularly interested in systematic evaluation of DFT performance in chemical reactions mediated by various transition metals, recently we have done a series of work on DFT performance assessment for barrier calculations of transition-metal-mediated reactions.[115−117,120−122] Previous efforts from other research groups and ours have led to DFT calibration studies covering a few 4d and 5d transition metals, including group 4 (Zr),[120] group 7 (Re),[121] group 8 (Ru),[117,126−129] group 9 (Rh, Ir),[110,115,116,126,130] and group 10 (Pd, Pt).[109,111−116,123,131,132] and group 11 (Au).[108,115,122,124,125,133,134] Concerning group 6 metals, there are few available DFT calibration studies only on a specific oxo-transfer reaction catalyzed by DMSO reductase. By employing CCSD method as reference, Hofmann assessed the performances of some DFT methods for geometry optimization and relative energy calculation, for which it was found that geometry optimizations were not much affected by employed DFs, but the computed relative energies depended highly on the DFs used for the energy computation.[94] Very recently Ryde and his co-workers explored the density-functional and basis set effects by referring to the local coupled cluster (LCC) LCCSD(T0) method, and they found a severe dependence of computational results on a density functional and basis set.[84] These previous results warrant a systematic DFT calibration study for important group 6 transition metals Mo and W on the activation energies of their typical reactions, which, to the best of our knowledge, is still missing. Hence in this work, we present our systematic study on the performance of diverse functionals in calculating a variety of selected representative Mo/W-mediated reactions as shown in Scheme 1. Instead of exploring a new mechanism, the main purpose of this work is to get detailed information on the performance of diverse DFs; hence, the widely accepted or most potential mechanisms explored before have been used in this work. It is our aim that this work can provide the missing guide information for researchers to explore the chemistry of reactions mediated by Mo and W more accurately with DFT methods. To reduce the computational expense of very costly ab initio reference methods, without affecting the reaction mode, certain truncations in some of our computational model systems (reactions 2, 4, 5, and 7) compared with the ones actually used in experimental or previous DFT studies have to be done. For example, in reaction 7, methane and $CpW(CO)_2B(OH)_2$ have been used to replace pentane and $Cp^*W(CO)_2(Bpin)$ for an affordable computational expense in W-mediated C−H activation.

2. COMPUTATIONAL DETAILS

2.1. Density-Functional Methods. All DFT calculations were performed with the Gaussian 09 suite of programs.[137] Due to the good performance of the PBE0 hybrid functional in generating geometries for transition metal complexes,[112,122,138−142] for all reactions except reaction 2, the geometry optimizations of minima and transition states were performed with this

DOI: 10.1021/acs.jctc.5b00373
J. Chem. Theory Comput. 2015, 11, 4601−4614

functional with the cc-pVDZ[143]/cc-pV(D+d)Z[144] basis sets on the main group atoms of B, C, H, O, N/S, and P (the cc-pVDZ used for B, C, H, O, and N, and the cc-pV(D+d)Z basis set used for S and P), and the cc-pVDZ-PP[145,146] basis set on TM atoms (Mo, W). For reaction 2 of W-mediated acetylene hydration, since the position of residue Asp13 in the second shell of the W center has a strong impact on the reaction profile, and the fully optimized geometry would deviate far from the corresponding one in AH enzyme, we did not do partial geometry optimizations but adopted the structures partially optimized by Himo et al.,[75] and replaced the Asp13 and substituents on C═C of two molybdopterin guanine dinucleotide (MGD) cofactors by acetate anion and hydrogen atoms, respectively. Hydrogen atoms have been added to the truncated bonds for which the sp^3 and sp^2 C−H bond lengths were set to 1.095 and 1.088 Å, respectively. For brevity, in the following text we may use the abbreviations (A)DZ/TZ/QZ to generally refer to (augmented) double-ζ/triple-ζ/quadruple-ζ quality correlation consistent basis sets. To account for the scalar relativistic effect of Mo/W, the Stuttgart new relativistic energy-consistent small-core pseudopotential (PP) ECP28MDF/ECP60MDF[145,146] for Mo/W was used throughout this work. The optimized structures were characterized as minima or transition states by harmonic vibrational analysis with no or one proper imaginary frequency. Based on these optimized geometries, single-point calculations were performed by all functionals under calibration. Commonly used density functionals, including two pure GGA functionals (BP86,[147,148] OLYP[149,150]), two pure meta-GGA functionals (M06-L,[151] TPSS[152]), two hybrid GGA functionals (PBE0,[153−155] B3LYP[147,149,156]), four hybrid meta-GGA functionals (M06,[151,157] M06-2X,[151,157] TPSSh,[152] BMK[158]), three range-separated functionals (ωB97X,[159] CAM-B3LYP,[160] LC-ωPBE[161,162]), and two double-hybrid functionals (B2GP-PLYP,[163] B2-PLYP[164]) are assessed in this study.

Since previous DFT calculations for DMSO reductase by Ryde et al. had shown a large dependence of results on the quality of the basis set,[84] it is important to determine if our DFT calculations are free from significant basis set incompleteness problems or not. Hence we have done extensive basis set convergence test calculations using B3LYP functional for all reactions 1−7 in Scheme 1. To test the basis set convergence of single-point DFT calculations, we calculated barriers of all reactions shown in Scheme 1 by B3LYP functional, with TZ (cc-pVTZ/cc-pV(T+d)Z/cc-pVTZ-PP for B, C, H, O, N/S, P/Mo, and W) and QZ (cc-pVQZ/cc-pV(Q+d)Z/cc-pVQZ-PP for B, C, H, O, N/S, P/Mo, and W) basis sets. The results in Table S1 (see the SI) demonstrate that, except for the two reactions 2 and 3, differences between TZ and QZ results are no larger than around 0.2 kcal/mol, which indicates a good basis set convergence and guarantees a safe use of the QZ basis set for these reactions. For reactions 2 and 3, however, the maximum difference up to 1.7 kcal/mol between TZ and QZ results is a warning sign. This unusually large difference between TZ and QZ basis sets implies that the basis set incompleteness error (BSIE) for DFT methods could be of considerable size here, which is in contrast to the weak and negligible basis set dependence down to the TZ basis set level as found in many of our previous studies,[115,116,120−122,165−167] but concurs with the finding of Ryde et al. for reaction 3.[84] Hence we further did ATZ and AQZ calculations and found that for reactions 2 and 3a, augmented basis functions are important for basis set convergence and ATZ results almost converge by having a difference of below 0.2 kcal/mol from AQZ ones. For reaction 3b, QZ is still necessary to be used since the QZ result is only around 0.1 kcal/mol away from the AQZ one, while the ATZ result is comparatively much away from the AQZ result by about 0.5 kcal/mol. By using this combination of basis sets (ATZ for reactions 2 and 3a and QZ for the rest of the reactions), which is the final choice for all of the DFT calculations, we anticipate that our typical DFT basis set convergence in this work should reach the level of magnitude of about 0.2 kcal/mol.

To assess the effect of DFT empirical dispersion, we adopted DFT-D3 correction of Grimme with a zero short-range damping scheme (the original D3 damping scheme).[168,169] For ωB97X functional without DFT-D3 parameters, the empirical dispersion corrected functional ωB97XD designed by its original developers was used instead.[170]

2.2. Coupled Cluster Methods. Based on PBE0 optimized geometries, all single-point ab initio calculations employing coupled cluster (CC) methods (CCSD(T) and CCSD(T)-F12) were carried out with Molpro program package.[171] As an ab initio approach, CC calculation could be quite dependent on the degree of basis set completeness. In this regard, the recently developed explicitly correlated CC methods can alleviate the strong basis set dependence of the traditional CC methods.[172] This improvement enables one to use a relatively small basis set of augmented double-ζ quality to produce results with accuracy comparable to that of the traditional CC approach with a much larger basis set. Thus, the computational expense of CC calculations with a large basis set is effectively reduced. To determine whether BSIE can be greatly reduced by CCSD(T)-F12 method for Mo/W-containing systems of interest, we have performed a series of costly CCSD(T) and CCSD(T)-F12 calculations for the relatively smaller system of Mo/W-mediated olefin epoxidation (reaction 6 in Scheme 1). These highly costly calculations are too expensive to be done for any other reactions in Scheme 1. The CCSD(T)-F12 approach used throughout this work employs the CCSD(T)-F12b method with the diagonal fixed amplitude 3C(FIX) *Ansatz*.[172,173] T1 diagnostic calculations for CCSD(T) have also been done to test the multiconfigurational character of our reactions under study. All tested T1 diagnostic values are below 0.05, which according to the common experience means that the multiconfigurational characters are not serious (see Table S2 of the SI). These results imply that the CCSD(T) calculations are reliable for these closed-shell systems under study.

First, for valence-only correlated CC calculations, we performed extrapolations for the complete basis set (CBS) limit at the CCSD(T) and CCSD(T)-F12b levels. These calculations employed ADZ and ATZ basis sets (nonaugmented basis for all H atoms, which was recommended before to be sufficiently accurate in CCSD(T)-F12 calculation)[172] to extrapolate to CCSD(T)-F12b/CBS and CCSD(T)/CBS values, the former one as the most accurate reference here. The CCSD(T)-F12b/CBS data were obtained according to the Schwenke's two-point CBS limit extrapolation scheme,[174] with CCSD-F12b correlation energy and perturbative triples contribution (T) extrapolated with eq 1 separately.

$$E_{\mathrm{corr},n} = E_{\mathrm{corr,CBS}} + \frac{A}{n^{\mathrm{pow}}} \tag{1}$$

The optimal parameter "pow" in CBS limit extrapolations was chosen to be 2.48307 for CCSD-F12b and 2.7903 for (T) contribution, which was determined by Hill et al. for ADZ-ATZ

DOI: 10.1021/acs.jctc.5b00373
J. Chem. Theory Comput. 2015, 11, 4601−4614

extrapolation.[175] The Hartree−Fock CBS limit in the CCSD-(T)-F12b/CBS value was not obtained from extrapolation but was approximated by the SCF+CABS-singles energy[176] calculated with the largest basis set (ATZ) used in CCSD-(T)-F12b calculations. Unlike CCSD, there is no direct F12 correction to the perturbative triples contribution (T). Without taking the default setting of Molpro, we did not scale (T) energy by a factor of MP2-F12/MP2 in all CCSD(T)-F12b calculations. In CCSD(T)-F12b calculations, without further specification, density fitting (DF) of the Fock and exchange matrices employed the auxiliary basis sets of def2-AQZVPP/JKFIT[177,178] for Mo/W and aug-cc-pVTZ/JKFIT[179,180] for the rest of the atoms (cc-pVTZ/JKFIT instead used for H), while DF of the other two-electron integrals and resolution of the identity (RI) approximation adopted aug-cc-pVTZ-PP/MP2FIT[181,182] for Mo/W and aug-cc-pVTZ/MP2FIT[183] for the rest of the atoms (cc-pVTZ/MP2FIT instead used for H). The value of the geminal Slater exponent in these valence-only correlated CCSD(T)-F12b calculations as well as in the core−valence correlated CCSD(T)-F12b calculations introduced later was chosen to be 1.4 a_0^{-1}, the same as the previous computational practices.[120,126,184]

The CCSD(T)/CBS data were obtained according to the two-point CBS limit extrapolation scheme as shown in eq 2 for total electronic energy,[185] which was found recently to be relatively superior to alternative extrapolation schemes.[186] To explore the effect of augmented (diffuse) basis functions, with CCSD(T) method, we also tested DZ and TZ basis sets, the CBS limit of which was also obtained from eq 2.

$$E_{\mathrm{toatl},n} = E_{\mathrm{toatl,CBS}} + \frac{A}{(n+1/2)^4} \tag{2}$$

The calculated reaction barriers $\Delta E^{\ddagger}$ (kcal/mol) for Mo/W-mediated olefin epoxidation with the CCSD(T) and CCSD(T)-F12b methods at various levels are presented in Table 1. The large difference between CCSD(T)/CBS results with ADZ-ATZ and DZ-TZ basis set pairs shows that the augmented basis functions have an apparent influence on the calculated results. Thus, augmented basis sets should be used in this work for the coupled cluster calculations. The CCSD(T)-F12b/ADZ $\Delta E^{\ddagger}_{\mathrm{val}}$ results in Table 1 are within 0.45 kcal/mol away from the reference CCSD(T)-F12b/CBS values, indicating an acceptable balance between computational accuracy and cost in the former approach. It is notable that the CCSD(T)/CBS(ADZ-ATZ) extrapolation result also generates quite accurate results. Considering the balance between computational cost and accuracy, for the valence-only correlated computations in this work, our method of choice is the CCSD(T)-F12b method with ADZ basis set (DZ for H).

Second, for the Mo/W 4s4p/5s5p outer core−valence correlation corrections, we also calculated their effect by using CCSD(T)-F12 method. The basis set used here for Mo/W was cc-pwCVDZ-PP designed especially for core−valence correlation treatment,[145] and DZ basis set for the rest of the atoms (abbreviated as wDZ totally; wTZ was defined similarly by replacing the double-ζ basis set to the corresponding triple-ζ basis set). To test if CCSD(T)-F12/wDZ is accurate enough with respect to the BSIE issue, we tested Mo/W-medidated olefin epoxidation reactions (reaction 6 in Scheme 1) by calculating CCSD(T)/CBS values derived from wDZ and wTZ two-point CBS limit extrapolation with eq 2. For a basis set, the outer core−valence correlation correction for activation energy is obtained by subtracting the barrier without core−valence

Table 1. Calculated Valence-Only Correlated Reaction Barriers $\Delta E^{\ddagger}_{\mathrm{val}}$ (kcal/mol) for Mo/W-Mediated Olefin Epoxidations (Reaction 6) from CCSD(T) and CCSD(T)-F12b Methods at Various Levels

reaction	CCSD(T)/DZ	CCSD(T)/TZ	CCSD(T)/CBS(DZ-TZ)	CCSD(T)/ADZ	CCSD(T)/ATZ	CCSD(T)/CBS(ADZ-ATZ)	CCSD(T)-F12b/ADZ	CCSD(T)-F12b/ATZ	CCSD(T)-F12b/CBS(ADZ-ATZ)
6 (Mo)	15.94	18.08	18.83	12.85	16.11	17.26	17.25	17.24	17.10
6 (W)	13.90	16.15	16.95	11.24	14.41	15.53	15.64	15.43	15.19

DOI: 10.1021/acs.jctc.5b00373
J. Chem. Theory Comput. 2015, 11, 4601−4614

Table 2. 4s4p/5s5p Outer Core−Valence Correlation Corrections $\Delta\Delta E^{\ddagger}_{nsnp}$ (kcal/mol) on Activation Energies of Mo/W-Mediated Olefin Epoxidations (Reaction 6)

reaction	CCSD(T)/wDZ	CCSD(T)/wTZ	CCSD(T)/CBS	CCSD(T)-F12/wDZ
6 (Mo)	−0.35	−0.11	−0.03	0.13
6 (W)	−0.23	−0.07	−0.01	0.13

correlation from the barrier with core−valence correlation, both calculated with the same basis set. The results in Table 2 show that the core−valence correlation corrections calculated at the CCSD(T)-F12/wDZ level differ from the corresponding CCSD(T)/CBS values by less than 0.2 kcal/mol, which is apparently better than the CCSD(T)/wDZ values obtained at about the same computational expense and is just slightly inferior to the computationally much more expensive CCSD(T)/wTZ results. As a result of the balance between accuracy and computational cost, CCSD(T)-F12/wDZ calculations were employed in core−valence electron correlation correction ($\Delta\Delta E^{\ddagger}_{nsnp}$) calculations to alleviate the potential BSIE problem.[172,173]

In the CCSD(T)-F12b calculations for outer core−valence correlation corrections, the auxiliary basis sets of def2-QZVPP/JKFIT for Mo/W and cc-pVTZ/JKFIT for the rest of the atoms were adopted for density fitting of the Fock and exchange matrices, while DF of the other two-electron integral and resolution of the identity approximation employed cc-pwCVTZ-PP/MP2FIT[182,187] for Mo/W and cc-pVTZ/MP2FIT for the rest of the atoms.

Our final reference values of activation energy $\Delta E^{\ddagger}_{final}$ were obtained as the sum of valence-only electron correlation result ($\Delta E^{\ddagger}_{val}$) and Mo/W *nsnp* ($n$ = 4 for Mo; n = 5 for W) core−valence correlation correction ($\Delta\Delta E^{\ddagger}_{nsnp}$), as shown in eq 3.

$$\Delta E^{\ddagger}_{final} = \Delta E^{\ddagger}_{val} + \Delta\Delta E^{\ddagger}_{nsnp} \quad (3)$$

The $\Delta E^{\ddagger}_{val}$ value was obtained from the valence-only correlated CCSD(T)-F12b/ADZ calculation, and $\Delta\Delta E^{\ddagger}_{nsnp}$ value was obtained from CCSD(T)-F12b/wDZ core−valence correlation correction calculation.

In this study, nonscalar relativistic effect from spin−orbit coupling (SOC) is not considered in both ab initio and DFT calculations. This is primarily due to the DFT calibration scope of this study, and the SOC effect is not relevant to comparison between ab initio and DFT methods as long as the reaction pathway is not changed by SOC. In addition, in our previous study for closed-shell reaction systems containing even heavier transition metals (Ir, Pt), we found that SOC only has a quite small effect (less than about 1 kcal/mol) to the reaction barriers.[165] Thus, SOC effect is likely to be unimportant in these closed-shell systems under study containing the lighter Mo and W transition metals.

3. RESULTS AND DISCUSSION

3.1. Reference Coupled Cluster Calculations. The reference activation energies of the seven types of reactions in Scheme 1 are shown in Table 3. Notably, in the olefin metathesis reactions 4 for both Mo and W, the first addition step of olefin to metal−carbene to form a metal−cyclobutane ring has a very small and even negative barrier. This phenomenon is just a reflection of the small magnitude of this barrier, which sometimes can even lead to "disappearance" of the corresponding transition state in olefin metathesis reaction, as known also in the case of Ru-mediated olefin metathesis studied by Truhlar, Grimme, and their co-workers.[127,128]

Table 3. CCSD(T)-F12 Calculated $\Delta E^{\ddagger}_{val}$, $\Delta\Delta E^{\ddagger}_{nsnp}$ (n = 4 for Mo, n = 5 for W), and $\Delta E^{\ddagger}_{final}$ for All Mo/W-Mediated Reactions in Scheme 1 (kcal/mol)

reaction	$\Delta E^{\ddagger}_{val}$	$\Delta\Delta E^{\ddagger}_{nsnp}$	$\Delta E^{\ddagger}_{final}$
1 (Mo)	25.16	−0.15	25.02
2 (W)	8.72	−0.20	8.52
3a (Mo)	18.37	0.29	18.66
3b (Mo)	13.78	−0.25	13.54
4a (Mo)	0.52	−0.43	0.09
4b (Mo)	14.22	0.47	14.69
4a (W)	−0.39	−0.23	−0.61
4b (W)	17.5	0.37	17.87
5a (W)	4.3	−0.03	4.27
5b (W)	18.92	0.83	19.75
6 (Mo)	17.25	0.13	17.38
6 (W)	15.64	0.13	15.77
7 (W)	8.77	−0.21	8.55

As shown in Table 3, the absolute values of the Mo 4s4p core−valence electron-correlation corrections $\Delta\Delta E^{\ddagger}_{4s4p}$ are quite small, being less than 0.5 kcal/mol, and the same is true for W 5s5p core−valence electron correlation corrections $\Delta\Delta E^{\ddagger}_{5s5p}$ except for the second step of alkyne metathesis with a slightly larger value ($\Delta\Delta E^{\ddagger}_{5s5p}$ = 0.83 kcal/mol for reaction 5b). These small magnitudes of all 4s4p/5s5p core−valence correlation corrections in this work are generally analogous to our previous core−valence correlation effect calculations for other early, middle, and late transition metals (Zr, Ru, Rh, Ir, Pt, and Re).[116,117,120,165]

Finally, for reaction 3a, our calculated CCSD(T)-F12 barrier ($\Delta E^{\ddagger}_{val}$ = 18.4 kcal/mol) is much larger than the previous LCCSD(T0) result of Ryde et al.[84] (2.3 kcal/mol) by more than 16 kcal/mol. After careful analysis and test, we found that this big difference is mainly due to the different ways to measure the barrier. In our case, the reactant complex was used as zero point to measure the barrier, while in the work of Ryde et al., the separated reactants (with respect to the Mo active center and DMSO substrate) was used. Using our model and the separated reactants, the barrier $\Delta E^{\ddagger}_{val}$ was calculated to be 2.1 kcal/mol, which is very close to the LCCSD(T0) result of 2.3 kcal/mol by Ryde et al.[84] So our barrier for reaction 3a measured from reactant complex is not comparable with that of Ryde et al.[84] measured from separated reactants. For reaction 3b, both using its reactant complex as zero point to measure the barrier, our calculated barrier ($\Delta E^{\ddagger}_{val}$ = 13.8 kcal/mol) is much closer to the corresponding LCCSD(T0) value (15.5 kcal/mol) from Ryde et al.[84] The relatively small difference of 1.7 kcal/mol for reaction 3b between our CCSD(T)-F12 result and that of Ryde et al. could come from many different calculation settings between the two works, including geometry optimization method, model truncation, basis set, and ab initio methodology difference (LCCSD(T0) vs CCSD(T)-F12). For this last point of LCC vs canonical CC issue, it is notable that their results sometimes can differ by more than 1 kcal/mol as shown in our previous work.[115] Furthermore, the calculated

DOI: 10.1021/acs.jctc.5b00373
J. Chem. Theory Comput. 2015, 11, 4601−4614

$\Delta E^{\ddagger}_{final}$ (13.5 kcal/mol) of reaction 3b is consistent with experimentally determined activation enthalpy (14.9 kcal/mol) in DMSO reductase[188] (reaction 3b was previously proposed to be rate-limiting step in reaction 3,[67,71] which is confirmed here by having TS of much higher energy than that of reaction 3a).

3.2. DFT Performance Assessment. To find whether one or more functionals are uniformly better than the others in barrier calculations of Mo/W-mediated reactions, we assessed the performances of all 15 DFT methods under calibration. Taking $\Delta E^{\ddagger}_{final}$ values in Table 3 as reference, the statistical analysis of the mean signed (MSD) and unsigned (MUD) deviations of various DFT methods are summarized in Table 4 and Table 5 and depicted in Figure 1.

3.2.1. Activation Energies of Mo- and W-Mediated Reactions. As shown in Table 4, among all functionals under assessment there are four DFs (values in bold) whose MUDs over all Mo-mediated reactions are below 2 kcal/mol (B2GP-PLYP, M06, B2-PLYP, and B3LYP). In addition to these four DFs, TPSSh also performs well by having a MUD(Mo) just slightly over 2 kcal/mol (2.12 kcal/mol). On the contrary, LC-ωPBE, ωB97X, BP86, BMK, and OLYP produce apparently larger MUDs(Mo) exceeding around 4 kcal/mol for Mo-mediated reactions. Therefore, their use in Mo-mediated reactions is not recommended.

For all W-mediated reactions, we identify the following four best performing DFs with MUDs(W) below 2 kcal/mol (B2GP-PLYP, M06, B2-PLYP, and TPSSh). Besides, B3LYP and CAM-B3LYP are also notable due to their low MUDs(W) just slightly over 2 kcal/mol (2.31 and 2.28 kcal/mol). Interestingly, we found that among the best performing DFs, almost all (B2GP-PLYP, M06, B2-PLYP, B3LYP, and TPSSh) are shared by Mo- and W-mediated reactions. This consistent good performance in both Mo- and W-mediated reactions from the following five DFs, i.e., B2GP-PLYP, M06, B2-PLYP, TPSSh, and B3LYP as demonstrated clearly by their MUDs(Mo+W) below about 2 kcal/mol shown in Table 4, is the prerequisite for getting commonly suitable DFs for Mo- and W-mediated reactions. Concerning the worst performing DFs in W-mediated reactions, consistent performance compared with that in Mo-mediated reactions is also apparent, with the same DFs of LC-ωPBE, ωB97X, BP86, BMK, and OLYP having the five largest MUDs(W). However, for these five DFs, MUDs(W) are generally smaller than the corresponding MUDs(Mo), indicating that W-mediated reactions are less demanding in accurate barrier calculation than Mo-mediated reactions.

Combining both Mo- and W-mediated reactions, the five best performing DFs have MUDs below about 2 kcal/mol, in the performance order of B2GP-PLYP < M06 < B2-PLYP < TPSSh < B3LYP (in MUD-increasing order). The maximum errors of all 15 tested DFTs come from reactions 3b, 5, and 6 as shown in Table 4 (values in bold), which all have metals in their highest valent VI formal oxidation state.

3.2.2. Effects of DFT Empirical Dispersion Correction. All of the deviations with DFT empirical dispersion correction included are collected in Table 5 and depicted in Figure 1b,d. Before we discuss the detailed effects of DFT empirical dispersion correction for Mo/W-mediated reactions, it is notable that M06 series DFs are almost not affected by DFT-D3 corrections (the MUDs change by less than 0.09 kcal/mol), which is consistent with the observations in our previous work for other transition metals.[115−117,122] This is presumably due to the parametrization of these DFs to account for dispersion interactions to a certain extent.

With DFT-D3 correction, for Mo-mediated reactions, functionals of best performance with MUDs below 2 kcal/mol are B2GP-PLYP < M06 < B3LYP < B2-PLYP (in MUD-increasing order). These four DFs are the same with the four best performing DFs without DFT-D3 correction, i.e., B2GP-PLYP < M06 < B2-PLYP < B3LYP. For Mo-mediated reactions, as seen from comparison between panels a and b of Figure 1, except for seven functionals (BP86, TPSS, TPSSh, M06, M06-2X, B2-PLYP, and B2GP-PLYP), the magnitudes of MUDs after taking account of DFT empirical dispersion correction decreased more or less compared with the corresponding magnitudes of MUDs without empirical dispersion correction. The most notable improvements come from BMK, CAM-B3LYP, ωB97X, and LC-ωPBE. After including DFT empirical dispersion correction, the corresponding MUDs decrease by 1.19, 0.61, 1.64, and 0.64 kcal/mol, respectively. Among the seven functionals with increased MUDs, none of their MUDs increase by more than 0.7 kcal/mol, which is tiny in the world of dispersion corrections for larger systems.

With DFT-D3 correction, for W-mediated reactions, functionals of best performance with MUD less than 2 kcal/mol are B2GP-PLYP < M06 < CAM-B3LYP < B2-PLYP < B3LYP (in MUD-increasing order), which can be compared to the corresponding order of functionals before adding DFT-D3 correction, B2GP-PLYP < M06 < B2-PLYP < TPSSh. For W-mediated reactions, after including DFT empirical dispersion correction, eight of the tested functionals (B3LYP, BMK, OLYP, CAM-B3LYP, PBE0, ωB97X, LC-ωPBE, and B2GP-PLYP) performed apparently better. The most notable improvements come from B3LYP, BMK, OLYP, CAM-B3LYP, and ωB97X. After including DFT empirical dispersion correction, the corresponding MUDs decrease by 0.57, 0.82, 0.59, 0.90, and 0.88 kcal/mol, respectively. Benefiting from this, the MUDs of B3LYP-D3 and CAM-B3LYP-D3 decrease to below 2 kcal/mol. Among the five DFs (BP86, TPSS, TPSSh, M06, and B2-PLYP) with increased MUDs after including DFT-D3 correction, similar to the Mo-mediated reactions, all changes from DFT-D3 correction are small, and none of their MUDs increases by more than 0.9 kcal/mol. Considering also that more bulky reaction systems than the reaction models under study here may bring larger dispersion corrections, empirical dispersion correction is recommended for both Mo- and W-mediated DFT barrier calculations.

Combining both Mo- and W-mediated reactions, four DFs after including DFT empirical dispersion correction have MUDs below 2 kcal/mol, in the performance order of B2GP-PLYP < M06 < B2-PLYP < B3LYP (in MUD-increasing order). The maximum errors of all 15 tested DFTs come from reactions 1, 3b, 4, 5, and 6 as shown in Table 5 (values in bold), which all have metals in their highest valent VI formal oxidation state.

3.2.3. Comparison to Previous DFT Calibration for Related Reactions of Other Metals. 3.2.3.1. Olefin/Alkyne Metathesis. Previously, Ru-mediated olefin metathesis reactions with well-known Grubbs first- and second-generation catalysts have been explored for DFT calibration purpose respectively by Grimme, Truhlar, and their co-workers,[127,128] with QCISD(T) and CCSD(T) methods employed as the respective reference methods. In order to compare more directly with our Mo/W-mediated olefin metathesis model, here we focus on the rate-limiting steps of the dissociative trans-pathway in Ru cases. The data of shared DFs under calibration in Ru/Mo/W-mediated olefin metathesis (B3LYP, PBE0, M06, M06-L, OLYP, BP86, TPSS, TPSSh, B2-PLYP, and B2GP-PLYP) have

DOI: 10.1021/acs.jctc.5b00373
J. Chem. Theory Comput. 2015, 11, 4601−4614

Table 4. Deviations of DFT-Computed Activation Energies (without DFT Empirical Dispersion Correction) of Mo- and W-Mediated Reactions from the Reference $\Delta E^{\ddagger}_{final}$ Data (kcal/mol)[a]

reaction	B3LYP	BMK	M06	M06- 2X	M06L	OLYP	CAM- B3LYP	BP86	PBE0	TPSS	TPSSh	ωB97X	B2-PLYP	B2GP- PLYP	LC- ωPBE
1 (Mo)	−0.16	−0.89	−0.63	0.44	−1.52	−4.33	1.45	−8.23	−5.07	−5.18	−3.86	3.81	0.67	2.55	1.41
3a (Mo)	2.64	1.83	0.05	0.02	−2.15	5.41	3.01	1.26	2.05	0.61	1.13	2.92	0.95	0.82	3.43
3b (Mo)	−1.28	**9.78**	1.29	**9.33**	−4.46	−6.37	5.83	**-10.27**	1.21	**-9.59**	−5.13	9.80	**-3.23**	0.69	11.20
4a (Mo)	2.72	1.15	0.98	2.44	1.97	2.05	2.32	−0.17	−0.48	−0.51	−0.39	2.56	0.58	−0.03	0.32
4b (Mo)	−1.19	4.98	1.11	0.45	0.94	1.48	1.27	−0.08	3.25	−0.55	0.49	3.25	−0.71	0.09	7.05
6 (Mo)	1.74	6.15	**2.62**	8.69	−4.40	2.96	**6.86**	−6.08	4.01	−5.75	−1.75	**10.07**	−2.40	−0.60	**14.03**
MSD(Mo)	0.82	3.83	0.90	3.56	−1.60	0.20	3.46	−3.93	0.83	−3.50	−1.59	5.40	−0.69	0.59	6.24
MUD(Mo)	**1.69**	4.13	**1.12**	3.56	2.57	3.76	3.46	4.35	2.68	3.70	2.12	5.40	**1.43**	**0.80**	6.24
2 (W)	4.00	1.98	0.60	−1.16	−0.57	5.71	2.34	−1.96	−1.45	−1.81	−1.32	2.12	0.26	**2.58**	0.05
4a (W)	1.61	0.8	0.73	1.66	1.26	0.93	1.43	0.01	−0.21	−0.18	−0.12	1.54	0.41	0.1	0.29
4b (W)	−2.17	5.08	0.7	0.6	−0.24	0.11	1.06	−1.37	2.81	−1.77	−0.43	3.66	−1.53	−0.6	7.76
5a (W)	**4.28**	1.44	−1.68	−1.56	−2.67	**8.07**	3.39	1.93	1.43	1.25	1.38	1.37	2.03	1.33	1.78
5b (W)	−1.75	9.38	2.04	−2.46	**5.46**	3.95	0.05	5.88	**8.71**	5.84	**6.12**	1.93	−1.92	−1.21	7.37
6 (W)	0.58	6.20	2.23	8.83	−4.31	1.26	5.77	−7.22	2.73	−6.91	−2.98	9.34	−2.83	−1.03	12.79
7 (W)	1.77	3.01	0.32	2.47	1.72	−1.81	1.91	−1.97	−1.26	−0.44	−0.04	1.41	0.26	−0.09	−0.35
MSD(W)	1.19	3.98	0.71	1.20	0.09	2.60	2.28	−0.67	1.82	−0.57	0.37	3.05	−0.48	0.15	4.24
MUD(W)	2.31	3.98	**1.19**	2.68	2.32	3.12	2.28	2.90	2.66	2.60	**1.77**	3.05	**1.32**	**0.99**	4.34
MSD(Mo+W)	1.01	3.91	0.80	2.29	−0.69	1.49	2.82	−2.17	1.37	−1.92	−0.53	4.14	−0.57	0.35	5.16
MUD(Mo+W)	2.02	4.05	**1.15**	3.08	2.44	3.42	2.82	3.57	2.67	3.11	**1.93**	4.14	**1.37**	**0.90**	5.22

[a]MUD values less than 2.0 kcal/mol, and maximum absolute deviation from each DF for all reactions, are denoted in bold.

DOI: 10.1021/acs.jctc.5b00373
J. Chem. Theory Comput. 2015, 11, 4601−4614

Table 5. Deviations of DFT-Computed Activation Energies (with DFT Empirical Dispersion Correction) of Mo- and W-Mediated Reactions from the Reference $\Delta E^{\ddagger}_{final}$ Data (kcal/mol)[a]

reaction	B3LYP	BMK	M06	M06-2X	M06L	OLYP	CAM- B3LYP	BP86	PBE0	TPSS	TPSSh	ωB97XD	B2-PLYP	B2GP- PLYP	LC- ωPBE
1 (Mo)	−0.03	−0.78	−0.57	0.48	−1.47	−6.51	1.58	−8.16	−4.97	−5.13	−3.77	1.54	0.77	**2.62**	1.54
3a (Mo)	1.63	−0.07	0.43	0.08	−2.06	0.64	2.24	0.38	1.67	0.23	0.60	3.57	0.20	0.20	2.64
3b (Mo)	−2.48	8.46	1.21	**9.33**	−4.46	**-8.94**	5.06	−11.70	0.52	**-10.60**	**-6.10**	5.80	−3.87	0.23	10.37
4a (Mo)	2.37	0.54	1.08	2.45	1.98	0.22	2.04	−0.47	−0.63	−0.65	−0.58	1.65	0.32	−0.24	0.04
4b (Mo)	−1.93	4.13	1.03	0.42	0.9	0.95	0.71	−0.85	2.81	−1.07	−0.06	2.23	−1.15	−0.23	6.47
6 (Mo)	−0.33	3.64	**2.60**	8.69	−4.40	−3.50	**5.45**	−8.35	2.88	−7.28	−3.30	**7.76**	−3.58	−1.48	**12.53**
MSD(Mo)	−0.06	2.65	0.96	3.58	−1.58	−2.86	2.85	−4.86	0.38	−4.08	−2.20	3.76	−1.22	0.18	5.60
MUD(Mo)	**1.53**	2.94	**1.15**	3.58	2.55	3.46	2.85	4.98	2.25	4.16	2.40	3.76	**1.65**	**0.83**	5.60
2 (W)	1.55	−0.99	0.58	−1.11	−0.51	−2.35	0.68	−4.76	−2.78	−3.69	−3.18	0.88	−1.13	1.56	−1.71
4a (W)	1.52	0.59	0.80	1.67	1.27	0.13	1.35	−0.04	−0.23	−0.17	−0.14	1.02	0.32	0.02	0.21
4b (W)	**-2.93**	4.22	0.62	0.56	−0.29	−0.38	0.48	−2.18	2.36	−2.32	−0.99	2.31	−1.99	−0.93	7.16
5a (W)	1.56	−1.53	−1.93	−1.60	−2.73	1.42	1.52	−1.18	−0.16	−0.94	−0.76	0.75	0.53	0.25	−0.20
5b (W)	−1.82	**9.42**	1.94	−2.53	**5.38**	4.74	−0.01	5.66	**8.63**	5.65	6.01	2.86	−1.95	−1.22	7.30
6 (W)	−1.70	3.28	2.26	8.84	−4.30	−5.51	4.16	**-9.61**	1.50	−8.46	−4.61	7.11	**-4.20**	−2.05	11.09
7 (W)	1.05	2.15	0.32	2.48	1.74	−3.15	1.43	−2.80	−1.65	−1.00	−0.59	0.29	−0.14	−0.39	−0.85
MSD(W)	−0.11	2.45	0.65	1.19	0.08	−0.73	1.37	−2.13	1.10	−1.56	−0.61	2.17	−1.22	−0.39	3.29
MUD(W)	**1.73**	3.17	**1.21**	2.68	2.32	2.53	**1.38**	3.75	2.47	3.18	2.33	2.17	**1.47**	**0.92**	4.08
MSD(Mo+W)	−0.09	2.54	0.80	2.29	−0.69	−1.71	2.05	−3.39	0.77	−2.72	−1.34	2.91	−1.22	−0.13	4.35
MUD(Mo+W)	**1.64**	3.06	**1.18**	3.10	2.42	2.96	2.05	4.32	2.37	3.63	2.36	2.91	**1.55**	**0.88**	4.78

[a]MUD values less than 2.0 kcal/mol, and maximum absolute deviation from each DF for all reactions, are shown in bold.

DOI: 10.1021/acs.jctc.5b00373
J. Chem. Theory Comput. 2015, 11, 4601−4614

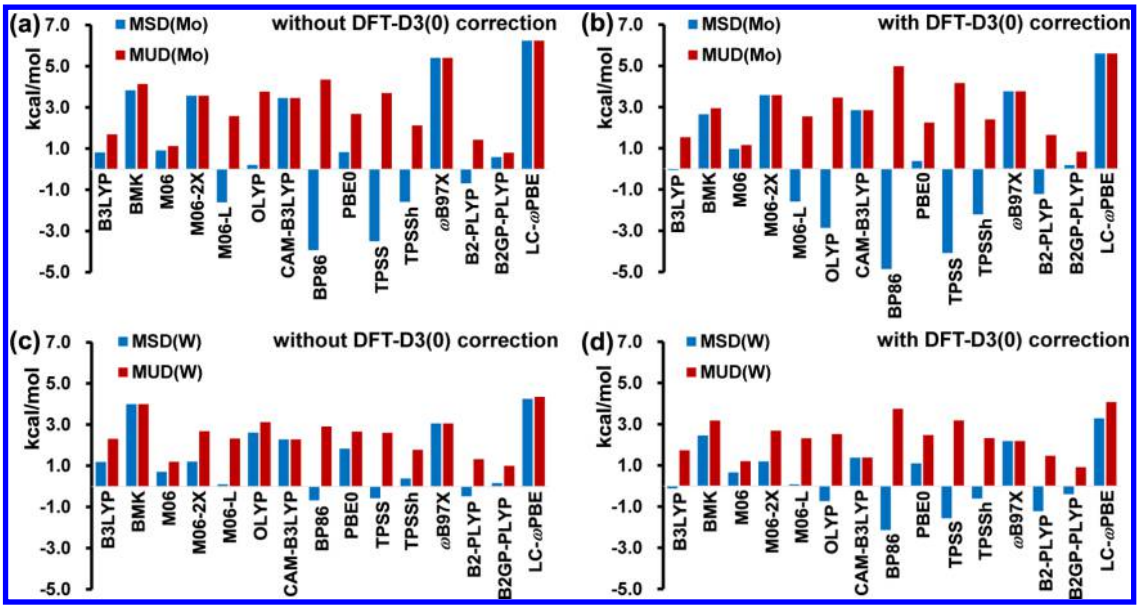

Figure 1. Mean unsigned and signed deviations (kcal/mol) of DFT-calculated activation energies taking $\Delta E^{\ddagger}_{\text{final}}$ as reference: (a) Mo-mediated reactions without DFT empirical dispersion correction; (b) Mo-mediated reactions with DFT empirical dispersion correction; (c) W-mediated reactions without DFT empirical dispersion correction; (d) W-mediated reactions with DFT empirical dispersion correction.

Table 6. Summary of Performance Assessment (Absolute Deviation or MUDs, kcal/mol) of Ten Commonly Used DFs in Activation Energy Calculations of Olefin/Alkyne Metathesis Reactions promoted by Ru, Mo, and W[a]

	B3LYP	PBE0	TPSSh	M06	M06-L	OLYP	BP86	TPSS	B2-PLYP	B2GP-PLYP	refs
Ru/olefin[b]	2.05		1.45				1.85		1.35		128
Ru/olefin[c]	1.85	3.10	1.57	0.99	1.31	1.15	0.32	1.26			127
Mo/olefin[d]	1.96	1.87	0.44	1.05	1.46	1.76	0.13	0.53	0.65	0.06	this work
W/olefin[e]	1.89	1.51	0.27	0.72	0.75	0.52	0.69	0.97	0.97	0.35	this work
W/alkyne[f]	3.01	5.07	3.75	1.86	4.07	6.01	3.91	3.54	1.98	1.27	this work

[a]For all of the data in the table, activation energies were calculated as the energy difference between the transition state and the preceding reactant complex, and DFT empirical dispersion corrections were not included. [b]The datum is MUD of two barriers in the trans-pathway collected from Table 4 in ref 128 (forward and backward steps from D_1^{trans} to D_2^{trans} through TS^{trans}). [c]The datum is MUD of two barriers in the trans-pathway collected from Table 3 in ref 127 (forward and backward steps from 3-trans to 4-trans through TS-trans). [d]The datum is MUD of reactions 4a (Mo) and 4b (Mo). [e]The datum is MUD of reactions 4a (W) and 4b (W). [f]The datum is MUD of reactions 5a (W) and 5b (W).

been collected in Table 6. As shown in Table 6, the absolute deviations of four commonly used DFs tested by Grimme et al.[128] for Grubbs first-generation Ru catalyst are all below about 2 kcal/mol from QCISD(T) reference (in the MUD-increasing order of B2-PLYP < TPSSh < BP86 < B3LYP), among which the smallest absolute deviation is 1.35 kcal/mol from B2-PLYP. For Grubbs second-generation Ru catalyst, the results of Truhlar et al.[127] shown in Table 6 demonstrate that all DFs have absolute deviations from CCSD(T) reference below 2 kcal/mol except PBE0, among which the best performances of absolute deviations below 1 kcal/mol are from BP86 and M06. In our Mo-mediated olefin metathesis reaction, the best performing DFs with MUDs less than 1 kcal/mol are B2GP-PLYP < BP86 < TPSSh < TPSS < B2-PLYP (in MUD-increasing order), while, for W, the order of best performing DFs with MUDs less than 1 kcal/mol is TPSSh < B2GP-PLYP < OLYP < BP86 < M06 < M06L < B2-PLYP ≈ TPSS (in MUD-increasing order).

Concerning W-mediated alkyne metathesis, none of the 10 DFs presented in Table 6 have MUDs below 1 kcal/mol. From Table 6 one can see that only M06, B2-PLYP, and B2GP-PLYP have kept all MUDs or deviations in olefin/alkyne metathesis reactions below around 2 kcal/mol. Thus, these DFs have stable performance in all presented data of Ru/Mo/W-mediated olefin/alkyne metathesis reactions.

3.2.3.2. Olefin Epoxidation. Recently, we found that the olefin epoxidation reaction similar to reaction 6 in Scheme 1 catalyzed by a high-valent organorhenium(VII) bisperoxo complex is quite different compared with other remediated reactions involving only a low-valent rhenium(I)/(III) formal oxidation state.[121] The DFTs calibration results of recatalyzed olefin epoxidation reaction show that many tested DFs (PBE, M06-2X, CAM-B3LYP, BP86, TPSS, ωB97X, and LC-ωPBE) perform very poorly to have quite large absolute deviations (from 5 to 15 kcal/mol, with and without DFT empirical dispersion correction), and only two DFs of B3LYP and B2GP-PLYP perform well with deviations smaller than around 2 kcal/mol. Except untested PBE, in reaction 6 of bisperoxo Mo(VI)/W(VI)-catalyzed olefin epoxidation, the deviations of poor performing DFs (M06-2X, CAM-B3LYP, BP86, TPSS, ωB97X, and LC-ωPBE) in recatalyzed olefin epoxidation reaction are still larger than around 4 kcal/mol. Interestingly, B3LYP and B2GP-PLYP perform well with deviations smaller than around 2 kcal/mol, in line with their good performances in corresponding remediated olefin epoxidation. Thus, it is not likely that the performances of DFs on olefin epoxidation

DOI: 10.1021/acs.jctc.5b00373
J. Chem. Theory Comput. 2015, 11, 4601−4614

Table 7. Summary of Performance Assessment (Absolute Deviation or MUDs, kcal/mol) of Four Hybrid DFs (B3LYP, PBE0, TPSSh, and M06) and One Double-Hybrid DF in C−H Activation Energy Calculations for Ru, Rh, Pd, Ir, Pt, Re, W, and Zr[a]

metals	B3LYP	PBE0	TPSSh	M06	B2-PLYP	mechanism[b]	refs
Pt, Ir	1.14 (0.94)	0.82 (0.94)	0.84 (0.87)	2.73 (2.71)	0.69 (0.73)	OA	115
Rh, Pd, Ir, Pt	1.17 (1.53)	2.27 (2.67)	3.35 (3.95)	5.04 (4.97)	2.26 (2.65)	OA	116
Ru, Rh	1.35 (0.67)	4.16 (3.78)	3.29 (2.76)	0.70 (0.74)	1.71 (1.34)	metathesis	126
Re	2.82 (2.73)	0.85 (1.14)	0.38 (0.45)	1.36 (1.42)[d]	3.45 (3.68)	OA and metathesis	121
W	1.77 (1.65)	1.26 (1.65)	0.04 (0.59)	0.32 (0.32)	0.26 (0.14)	metathesis	this work
Zr[c]	1.62 (0.79)	2.29 (2.74)	0.12 (0.73)	0.46 (0.46)	1.49 (1.01)	metathesis	120

[a]Values with DFT-D3 correction are inside parentheses. [b]OA represents oxidation addition mechanism; metathesis refers to σ-bond metathesis or other metathesis type mechanism. [c]Note that consistent with all the other data in the table, here activation energy was calculated as the difference between the transition state energy and the preceding reactant complex energy, though activation energy measured from separated reactants was also reported in ref 120. [d]In the listed averaged data over both σ-bond metathesis and oxidation addition mechanisms, here M06 has a much smaller absolute deviation for C−H activation via σ-bond metathesis mechanism (0.55/0.58 kcal/mol without/with DFT-D3) than that via oxidation addition mechanism (2.14/2.25 kcal/mol without/with DFT-D3).

catalyzed by bisperoxo organometallic catalysts depend on transition metal identity very much.

3.2.3.3. C−H Activation. In our previous DFT calibration work, the C−H activation process is often of special interest, for which we have explored different metals such as platinum group metals (Ru, Rh, Pd, Ir, and Pt),[115,116,126] middle transition metal (Re),[121] and early transition metal (Zr).[120] In these studies, C−H activations can be classified by two different mechanisms involved. One mechanism is oxidation addition (OA), in which the metal formal oxidation state is increased by 2; the other is of σ-bond metathesis type, in which the metal formal oxidation state is not affected. Concerning the early transition metal W-mediated C−H activation (reaction 7) involving σ-bond metathesis mechanism in the current work, among all the tested functionals, BMK/OLYP has the largest absolute deviation of 3.01/3.15 kcal/mol without/with DFT-D3 correction, as shown in Tables 4 and 5. Both with and without DFT-D3 correction, M06, TPSS, TPSSh, B2-PLYP, B2GP-PLYP, and LC-ωPBE have absolute deviations less than about 1 kcal/mol in C−H activation, among which, except TPSS and LC-ωPBE, the other DFs have absolute deviations less than 0.6 kcal/mol. With DFT empirical dispersion correction, ωB97XD also performs notably well with an absolute deviation of 0.29 kcal/mol.

In our previous work on late platinum group transition metals Ir and Pt for C−H activations via oxidation addition mechanism,[115] both with and without DFT-D3 correction, four DFs of TPSSh, B2-PLYP, B2GP-PLYP, and PBE0 have MUDs less than about 1 kcal/mol in C−H activation. For pincer complex systems, after exploring more late platinum group metals Rh and Pd in addition to Ir and Pt, the performancs of most DFs for C−H activations with oxidation addition mechanism deteriorate, while B3LYP notably keeps its performace, resulting in the lowest MUD of 1.17/1.53 without/with DFT-D3 correction (B3LYP is the only DF having MUD below 2 kcal/mol).[116] Concerning the C−H activations with σ-bond metathesis mechanism by platinum group transition metals Ru and Rh, recently we found that, with and without DFT-D3 correction, only M06 and CAM-B3LYP keep all absolute deviations below about 1 kcal/mol.[126] With DFT empirical dispersion correction, ωB97XD also performs notably quite well with absolute deviations below 0.8 kcal/mol. For middle transition metal Re, we have explored its C−H activations via both oxidation addition and σ-bond metathesis mechanisms, and we found that only four DFs of TPSS, TPSSh, B2GP-PLYP, and LC-ωPBE have absolute deviations below 1 kcal/mol both with and without DFT-D3 correction.[121] For C−H activation by early transition metal Zr via metathesis type mechanism, M06, TPSS, and TPSSh are the three DFs that have absolute deviations without DFT-D3 correction.[120,189] After DFT empirical dispersion correction, several more DFs improve their performances to reduce absolute deviations below about 1 kcal/mol, including B3LYP-D3, CAM-B3LYP-D3, B2-PLYP-D3, and B2GP-PLYP-D3.

For the four probably most widely used hybrid functionals B3LYP, PBE0, TPSSh, and M06, as well as the representative double-hybrid DF B2-PLYP, their performances in platinum group metals (Ru, Rh, Pd, Ir, and Pt),[115,116,126] middle transition metal (Re),[121] and early transition metal (Zr[120], W) systems are collected in Table 7. From Table 7 one can see that despite the fact that B3LYP often is not the best one with smallest deviations, it has the most stable performance; thus the errors in all explored systems are kept below around 3 kcal/mol. Another interesting phenomenon observed for the M06 functional is that it performs much better for σ-bond metathesis mechanism than for oxidation addition mechanism. This interesting difference between M06 and other DFs is noteworthy and may deserve future exploration.

3.2.4. Correlation Analysis for Trend of DFT Results. In addition to the DFT performance in barrier height value, due to the usefulness of barrier height trend to gain insight into chemical reactivity, exploring the trend performance of DFT-calculated barriers is also meaningful for DFT calculations. Having a good correlation between DFT barriers and reference values as a prerequisite, the slope of the correlation line can reflect the error in relative reaction barriers between different reactions that is useful in quantitatively describing the reactivity difference, and the intercept of the correlation line can measure the systematic barrier deviation by a certain DFT method. In order to explore this aspect of DFT performance, we separately plotted the correlations of barriers from 15 DFTs with the reference coupled cluster data $\Delta E^{\ddagger}_{\mathrm{final}}$ as shown in Figure 2 (without DFT dispersion correction) and Figure 3 (with DFT dispersion correction).

As shown in Figures 2 and 3, the correlations ($R^2 > 0.93$) of the best performing functionals involved all five of the best performing functionals (B2GP-PLYP, M06, B2-PLYP, B3LYP, and CAM-B3LYP) in MUDs. Except for these five best performing functionals, the correlation values of other tested functionals are all smaller than 0.93. Thus, more attention will be paid to these five functionals. From Figure 2, among these five functionals, three (B2GP-PLYP, M06, and B2-PLYP) have

DOI: 10.1021/acs.jctc.5b00373
J. Chem. Theory Comput. 2015, 11, 4601−4614

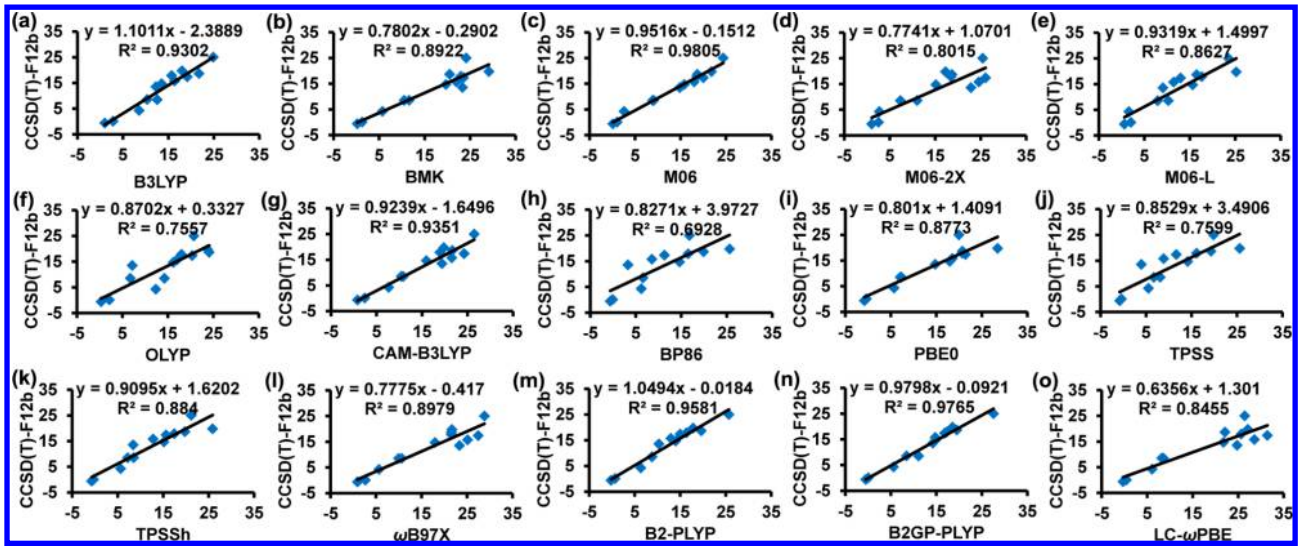

Figure 2. Correlations of the calculated barriers (kcal/mol) for all Mo/W-mediated reactions in Scheme 1 between $\Delta E^{\ddagger}_{\text{final}}$ and various DFT-calculated data without DFT empirical dispersion correction.

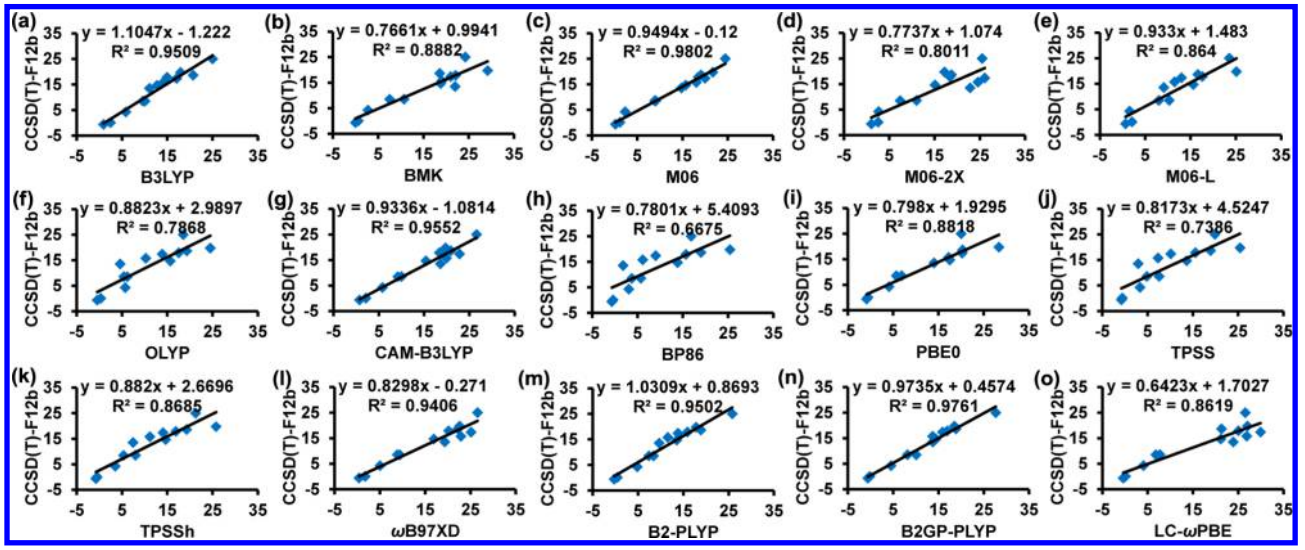

Figure 3. Correlations of the calculated barriers (kcal/mol) for all Mo/W-mediated reactions in Scheme 1 between $\Delta E^{\ddagger}_{\text{final}}$ and various DFT-calculated data with DFT empirical dispersion correction.

the correlation line slopes quite close to ideal 1.0 (absolute deviations within 0.06 from 1.0), and their intercepts of the correlation lines are also negligible (within 0.20 kcal/mol from ideal zero), indicating that barrier trend is well-followed and systematic deviations (underestimation/overestimation) of these functionals from accurate results are also small. After including DFT-D3 corrections, from Figure 3, the correlation line slopes of B2GP-PLYP, M06, and B2-PLYP remain quite close to the ideal 1.0 (absolute deviations within 0.06 from 1.0), and the correlation line intercept of M06 remains negligible (below 0.20 kcal/mol). However, the correlation line intercepts of B2GP-PLYP and B2-PLYP both increase somewhat from 0.09 and 0.02 kcal/mol to 0.46 and 0.87 kcal/mol, respectively.

4. CONCLUSIONS

In this work, by using the high-level coupled cluster CCSD(T)-F12 approach as a reference, we have assessed the performances of 15 frequently used DFT methods on barrier calculations of seven selected typical and important Mo/W-mediated enzymatic and organometallic reactions. We find that, with and without DFT-D3 correction, the best performing functionals for Mo-mediated reactions barrier height calculations (MUD less than 2 kcal/mol) include four functionals: B2GP-PLYP, M06, B3LYP, and B2-PLYP. For W-mediated reactions, B2GP-PLYP, M06, B2-PLYP, and TPSSh are the four best performing functionals (MUD less than 2 kcal/mol) without DFT-D3 correction. With DFT-D3 correction, however, B3LYP and CAM-B3LYP replace TPSSh to become the five best performing functionals (MUD less than 2 kcal/mol). Combining both Mo- and W-mediated reactions, four DFs of B2GP-PLYP, M06, B2-PLYP, and B3LYP can be uniformly recommended, with and without DFT empirical dispersion correction.

DFT empirical dispersion correction can improve the performances of many tested DFs, notably for B3LYP, CAM-B3LYP, ωB97X, BMK, OLYP, and LC-ωPBE. Compared with the often large DFT empirical dispersion correction in more bulky reaction systems, the absolute values of DFT empirical dispersion correction in our reaction models under study here are generally

DOI: 10.1021/acs.jctc.5b00373
J. Chem. Theory Comput. 2015, 11, 4601−4614

small. In general, we recommend the use of empirical dispersion correction in both Mo- and W-mediated DFT barrier calculations.

Considering both the trend of DFT results and the MUD value, with and without DFT empirical dispersion correction, double-hybrid functionals B2GP-PLYP and B2-PLYP and hybrid functional M06 perform better than other functionals tested and are our recommendation of DFs for both Mo- and W-mediated reactions.

■ ASSOCIATED CONTENT

Supporting Information

The Supporting Information is available free of charge on the ACS Publications website at DOI: 10.1021/acs.jctc.5b00373.

Three tables of computational results and Cartesian coordinates of all species (PDF)

■ AUTHOR INFORMATION

Corresponding Author

*E-mail: chenh@iccas.ac.cn.

Funding

This work was supported by the National Natural Science Foundation of China (NSFC, Grant Nos. 21290194, 21221002, and 21473215) and the Institute of Chemistry, Chinese Academy of Sciences.

Notes

The authors declare no competing financial interest.

■ REFERENCES

(1) Hille, R. *Chem. Rev.* **1996**, *96*, 2757−2816.
(2) Hille, R. *Arch. Biochem. Biophys.* **2005**, *433*, 107−116.
(3) Johnson, M. K.; Rees, D. C.; Adams, M. W. W. *Chem. Rev.* **1996**, *96*, 2817−2839.
(4) Hille, R. *Trends Biochem. Sci.* **2002**, *27*, 360−367.
(5) Majumdar, A.; Sarkar, S. *Coord. Chem. Rev.* **2011**, *255*, 1039−1054.
(6) Hille, R.; Hall, J.; Basu, P. *Chem. Rev.* **2014**, *114*, 3963−4038.
(7) Holm, R. H.; Solomon, E. I.; Majumdar, A.; Tenderholt, A. *Coord. Chem. Rev.* **2011**, *255*, 993−1015.
(8) Bevers, L. E.; Hagedoorn, P.-L.; Hagen, W. R. *Coord. Chem. Rev.* **2009**, *253*, 269−290.
(9) Moura, J. J.; Brondino, C. D.; Trincão, J.; Romão, M. J. *J. Biol. Inorg. Chem.* **2004**, *9*, 791−799.
(10) Mendel, R. R. *Dalton Trans.* **2005**, 3404−3409.
(11) Metz, S.; Thiel, W. *Coord. Chem. Rev.* **2011**, *255*, 1085−1103.
(12) Rosner, B. M.; Schink, B. *J. Bacteriol.* **1995**, *177*, 5767−5772.
(13) tenBrink, F.; Schink, B.; Kroneck, P. M. H. *J. Bacteriol.* **2011**, *193*, 1229−1236.
(14) Fürstner, A.; Davies, P. W. *Chem. Commun.* **2005**, 2307−2320.
(15) Hoveyda, A. H.; Zhugralin, A. R. *Nature* **2007**, *450*, 243−251.
(16) Chauvin, Y. *Angew. Chem., Int. Ed.* **2006**, *45*, 3740−3747.
(17) Bunz, U. H. F. *Acc. Chem. Res.* **2001**, *34*, 998−1010.
(18) Nicolaou, K. C.; Bulger, P. G.; Sarlah, D. *Angew. Chem., Int. Ed.* **2005**, *44*, 4490−4527.
(19) Dickman, M. H.; Pope, M. T. *Chem. Rev.* **1994**, *94*, 569−584.
(20) Waltz, K. M.; Hartwig, J. F. *Science* **1997**, *277*, 211−213.
(21) Grubbs, R. H. *Angew. Chem., Int. Ed.* **2006**, *45*, 3760−3765.
(22) Sergienko, V. S. *Crystallogr. Rep.* **2008**, *53*, 18−46.
(23) Heppekausen, J.; Fürstner, A. *Angew. Chem., Int. Ed.* **2011**, *50*, 7829−7832.
(24) Mougel, V.; Copéret, C. *Chem. Sci.* **2014**, *5*, 2475−2481.
(25) Conley, M. P.; Mougel, V.; Peryshkov, D. V.; Forrest, W. P., Jr.; Gajan, D.; Lesage, A.; Emsley, L.; Copéret, C.; Schrock, R. R. *J. Am. Chem. Soc.* **2013**, *135*, 19068−19070.
(26) Fürstner, A.; Guth, O.; Rumbo, A.; Seidel, G. *J. Am. Chem. Soc.* **1999**, *121*, 11108−11113.
(27) Weiss, K.; Michel, A.; Auth, E. M.; Bunz, U. H. F.; Mangel, T.; Müllen, K. *Angew. Chem., Int. Ed. Engl.* **1997**, *36*, 506−509.
(28) Hellbach, B.; Gleiter, R.; Rominger, F. *Synthesis* **2003**, 2535−2541.
(29) Bauer, E. B.; Hampel, F.; Gladysz, J. A. *Adv. Synth. Catal.* **2004**, *346*, 812−822.
(30) Fürstner, A.; Grela, K. *Angew. Chem., Int. Ed.* **2000**, *39*, 1234−1236.
(31) Fürstner, A.; Grela, K.; Mathes, C.; Lehmann, C. W. *J. Am. Chem. Soc.* **2000**, *122*, 11799−11805.
(32) Kozhevnikov, I. V. *Chem. Rev.* **1998**, *98*, 171−198.
(33) Neumann, R.; Cohen, M. *Angew. Chem., Int. Ed. Engl.* **1997**, *36*, 1738−1740.
(34) Burke, A. J. *Coord. Chem. Rev.* **2008**, *252*, 170−175.
(35) Müller, C.; Grover, N.; Cokoja, M.; Kühn, F. E. *Adv. Inorg. Chem.* **2013**, *65*, 33−83.
(36) Kühn, F. E.; Santos, A. M.; Herrmann, W. A. *Dalton Trans.* **2005**, 2483−2491.
(37) Lam, W. H.; Lin, Z. *Organometallics* **2003**, *22*, 473−480.
(38) Pamplin, C. B.; Legzdins, P. *Acc. Chem. Res.* **2003**, *36*, 223−233.
(39) Tsang, J. Y. K.; Fujita-Takayama, C.; Buschhaus, M. S. A.; Patrick, B. O.; Legzdins, P. *J. Am. Chem. Soc.* **2006**, *128*, 14762−14763.
(40) Wada, K.; Pamplin, C. B.; Legzdins, P.; Patrick, B. O.; Tsyba, I.; Bau, R. *J. Am. Chem. Soc.* **2003**, *125*, 7035−7048.
(41) Sawyer, K. R.; Cahoon, J. F.; Shanoski, J. E.; Glascoe, E. A.; Kling, M. F.; Schlegel, J. P.; Zoerb, M. C.; Hapke, M.; Hartwig, J. F.; Webster, C. E.; Harris, C. B. *J. Am. Chem. Soc.* **2010**, *132*, 1848−1859.
(42) Zhang, W.; Kraft, S.; Moore, J. S. *J. Am. Chem. Soc.* **2004**, *126*, 329−335.
(43) Zhang, W.; Moore, J. S. *J. Am. Chem. Soc.* **2005**, *127*, 11863−11870.
(44) Schrock, R. R.; Clark, D. N.; Sancho, J.; Wengrovius, J. H.; Rocklage, S. M.; Pedersen, S. F. *Organometallics* **1982**, *1*, 1645−1651.
(45) Wengrovius, J. H.; Sancho, J.; Schrock, R. R. *J. Am. Chem. Soc.* **1981**, *103*, 3932−3934.
(46) Schrock, R. R. *Chem. Commun.* **2013**, *49*, 5529−5531.
(47) Deraedt, C.; d'Halluin, M.; Astruc, D. *Eur. J. Inorg. Chem.* **2013**, *2013*, 4881−4908.
(48) Adam, W.; Mitchell, C. M.; Saha-Möller, C. R. *Eur. J. Org. Chem.* **1999**, *1999*, 785−790.
(49) Mimoun, H.; Seree de Roch, I.; Sajus, L. *Tetrahedron* **1970**, *26*, 37−50.
(50) Deubel, D. V.; Sundermeyer, J.; Frenking, G. *Eur. J. Inorg. Chem.* **2001**, *2001*, 1819−1827.
(51) Schulz, M.; Teles, J. H.; Sundermeyer, J.; Wahl, G. (BASF AG) WO Patent 1997010054 A1, 1995.
(52) Mkhalid, I. A. I.; Barnard, J. H.; Marder, T. B.; Murphy, J. M.; Hartwig, J. F. *Chem. Rev.* **2010**, *110*, 890−931.
(53) Zhang, S.-Y.; Zhang, F.-M.; Tu, Y.-Q. *Chem. Soc. Rev.* **2011**, *40*, 1937−1949.
(54) Johnson, K. R. D.; Hayes, P. G. *Chem. Soc. Rev.* **2013**, *42*, 1947−1960.
(55) Arockiam, P. B.; Bruneau, C.; Dixneuf, P. H. *Chem. Rev.* **2012**, *112*, 5879−5918.
(56) Debad, J. D.; Legzdins, P.; Lumb, S. A.; Batchelor, R. J.; Einstein, F. W. B. *J. Am. Chem. Soc.* **1995**, *117*, 3288−3289.
(57) Gisdakis, P.; Yudanov, I. V.; Rösch, N. *Inorg. Chem.* **2001**, *40*, 3755−3765.
(58) Wahl, G.; Kleinhenz, D.; Schorm, A.; Sundermeyer, J.; Stowasser, R.; Rummey, C.; Bringmann, G.; Fickert, C.; Kiefer, W. *Chem.-Eur. J.* **1999**, *5*, 3237−3251.
(59) Solans-Monfort, X. *Dalton Trans.* **2014**, *43*, 4573−4586.
(60) Rappe, A. K.; Goddard, W. A. *J. Am. Chem. Soc.* **1982**, *104*, 448−456.
(61) Poater, A.; Solans-Monfort, X.; Clot, E.; Copéret, C.; Eisenstein, O. *J. Am. Chem. Soc.* **2007**, *129*, 8207−8216.
(62) Tia, R.; Adei, E. *Dalton Trans.* **2010**, *39*, 7575−7587.

DOI: 10.1021/acs.jctc.5b00373
J. Chem. Theory Comput. 2015, 11, 4601−4614

(63) Smith, P. D.; Millar, A. J.; Young, C. G.; Ghosh, A.; Basu, P. *J. Am. Chem. Soc.* **2000**, *122*, 9298−9299.
(64) Thapper, A.; Deeth, R. J.; Nordlander, E. *Inorg. Chem.* **1999**, *38*, 1015−1018.
(65) Katz, T. J.; Mcginnis, J. *J. Am. Chem. Soc.* **1975**, *97*, 1592−1594.
(66) Sung, K. M.; Holm, R. H. *J. Am. Chem. Soc.* **2002**, *124*, 4312−4320.
(67) Tenderholt, A. L.; Hodgson, K. O.; Hedman, B.; Holm, R. H.; Solomon, E. I. *Inorg. Chem.* **2012**, *51*, 3436−3442.
(68) McNamara, J. P.; Joule, J. A.; Hillier, I. H.; Garner, C. D. *Chem. Commun.* **2005**, 177−179.
(69) Thapper, A.; Deeth, R. J.; Nordlander, E. *Inorg. Chem.* **2002**, *41*, 6695−6702.
(70) Webster, C. E.; Hall, M. B. *J. Am. Chem. Soc.* **2001**, *123*, 5820−5821.
(71) Tenderholt, A. L.; Wang, J.-J.; Szilagyi, R. K.; Holm, R. H.; Hodgson, K. O.; Hedman, B.; Solomon, E. I. *J. Am. Chem. Soc.* **2010**, *132*, 8359−8371.
(72) Otrelo-Cardoso, A. R.; da Silva Correia, M. A.; Schwuchow, V.; Svergun, D. I.; Romão, M. J.; Leimkühler, S.; Santos-Silva, T. *Int. J. Mol. Sci.* **2014**, *15*, 2223−2236.
(73) Santos-Silva, T.; Ferroni, F.; Thapper, A.; Marangon, J.; González, P. J.; Rizzi, A. C.; Moura, I.; Moura, J. J. G.; Romão, M. J.; Brondino, C. D. *J. Am. Chem. Soc.* **2009**, *131*, 7990−7998.
(74) Seiffert, G. B.; Ullmann, G. M.; Messerschmidt, A.; Schink, B.; Kroneck, P. M.; Einsle, O. *Proc. Natl. Acad. Sci. U.S.A.* **2007**, *104*, 3073−3077.
(75) Liao, R. Z.; Yu, J. G.; Himo, F. *Proc. Natl. Acad. Sci. U.S.A.* **2010**, *107*, 22523−22527.
(76) Deubel, D. V.; Sundermeyer, J.; Frenking, G. *J. Am. Chem. Soc.* **2000**, *122*, 10101−10108.
(77) Sharpless, K. B.; Townsend, J. M.; Williams, D. R. *J. Am. Chem. Soc.* **1972**, *94*, 295−296.
(78) Kisker, C.; Schindelin, H.; Rees, D. C. *Annu. Rev. Biochem.* **1997**, *66*, 233−267.
(79) Hille, R.; Rétey, J.; Bartlewski-Hof, U.; Reichenbecher, W.; Schink, B. *FEMS Microbiol. Rev.* **1998**, *22*, 489−501.
(80) Metz, S.; Wang, D.; Thiel, W. *J. Am. Chem. Soc.* **2009**, *131*, 4628−4640.
(81) Ha, Y.; Tenderholt, A. L.; Holm, R. H.; Hedman, B.; Hodgson, K. O.; Solomon, E. I. *J. Am. Chem. Soc.* **2014**, *136*, 9094−9105.
(82) McNamara, J. P.; Hillier, I. H.; Bhachu, T. S.; Garner, C. D. *Dalton Trans.* **2005**, 3572−3579.
(83) Hernandez-Marin, E.; Ziegler, T. *Can. J. Chem.* **2010**, *88*, 683−693.
(84) Li, J.-L.; Mata, R. A.; Ryde, U. *J. Chem. Theory Comput.* **2013**, *9*, 1799−1807.
(85) Vincent, M. A.; Hillier, I. H.; Periyasamy, G.; Burton, N. A. *Dalton Trans.* **2010**, *39*, 3816−3822.
(86) Antony, S.; Bayse, C. A. *Organometallics* **2009**, *28*, 4938−4944.
(87) Solans-Monfort, X.; Copéret, C.; Eisenstein, O. *J. Am. Chem. Soc.* **2010**, *132*, 7750−7757.
(88) Beer, S.; Hrib, C. G.; Jones, P. G.; Brandhorst, K.; Grunenberg, J.; Tamm, M. *Angew. Chem., Int. Ed.* **2007**, *46*, 8890−8894.
(89) Zhu, J.; Jia, G. C.; Lin, Z. Y. *Organometallics* **2006**, *25*, 1812−1819.
(90) Deubel, D. V.; Frenking, G.; Gisdakis, P.; Herrmann, W. A.; Rösch, N.; Sundermeyer, J. *Acc. Chem. Res.* **2004**, *37*, 645−652.
(91) Yudanov, I. V.; Di Valentin, C.; Gisdakis, P.; Rösch, N. *J. Mol. Catal. A: Chem.* **2000**, *158*, 189−197.
(92) Webster, C. E.; Fan, Y.; Hall, M. B.; Kunz, D.; Hartwig, J. F. *J. Am. Chem. Soc.* **2003**, *125*, 858−859.
(93) Herbert, M.; Montilla, F.; Álvarez, E.; Galindo, A. *Dalton Trans.* **2012**, *41*, 6942−6956.
(94) Hofmann, M. *J. Mol. Struct.: THEOCHEM* **2006**, *773*, 59−70.
(95) Hofmann, M. *Inorg. Chem.* **2008**, *47*, 5546−5548.
(96) Ackermann, L. *Chem. Rev.* **2011**, *111*, 1315−1345.
(97) Balcells, D.; Clot, E.; Eisenstein, O. *Chem. Rev.* **2010**, *110*, 749−823.
(98) Shaik, S.; Cohen, S.; Wang, Y.; Chen, H.; Kumar, D.; Thiel, W. *Chem. Rev.* **2010**, *110*, 949−1017.
(99) Cramer, C. J.; Truhlar, D. G. *Phys. Chem. Chem. Phys.* **2009**, *11*, 10757−10816.
(100) Rotzinger, F. P. *Chem. Rev.* **2005**, *105*, 2003−2037.
(101) Ziegler, T.; Autschbach, J. *Chem. Rev.* **2005**, *105*, 2695−2722.
(102) Noodleman, L.; Lovell, T.; Han, W. G.; Li, J.; Himo, F. *Chem. Rev.* **2004**, *104*, 459−508.
(103) Baik, M. H.; Newcomb, M.; Friesner, R. A.; Lippard, S. J. *Chem. Rev.* **2003**, *103*, 2385−2419.
(104) Niu, S. Q.; Hall, M. B. *Chem. Rev.* **2000**, *100*, 353−405.
(105) Siegbahn, P. E.; Blomberg, M. R. *Chem. Rev.* **2000**, *100*, 421−438.
(106) Torrent, M.; Solà, M.; Frenking, G. *Chem. Rev.* **2000**, *100*, 439−494.
(107) Dedieu, A. *Chem. Rev.* **2000**, *100*, 543−600.
(108) Moncho, S.; Brothers, E. N.; Janesko, B. G. *J. Phys. Chem. C* **2013**, *117*, 7487−7496.
(109) Oyedepo, G. A.; Wilson, A. K. *ChemPhysChem* **2011**, *12*, 3320−3330.
(110) Anoop, A.; Thiel, W.; Neese, F. *J. Chem. Theory Comput.* **2010**, *6*, 3137−3144.
(111) de Jong, G. T.; Bickelhaupt, F. M. *J. Chem. Theory Comput.* **2006**, *2*, 322−335.
(112) Quintal, M. M.; Karton, A.; Iron, M. A.; Boese, A. D.; Martin, J. M. *J. Phys. Chem. A* **2006**, *110*, 709−716.
(113) de Jong, G. T.; Geerke, D. P.; Diefenbach, A.; Solà, M.; Bickelhaupt, F. M. *J. Comput. Chem.* **2005**, *26*, 1006−1020.
(114) de Jong, G. T.; Geerke, D. P.; Diefenbach, A.; Bickelhaupt, F. M. *Chem. Phys.* **2005**, *313*, 261−270.
(115) Kang, R. H.; Lai, W. Z.; Yao, J. N.; Shaik, S.; Chen, H. *J. Chem. Theory Comput.* **2012**, *8*, 3119−3127.
(116) Lai, W. Z.; Yao, J. N.; Shaik, S.; Chen, H. *J. Chem. Theory Comput.* **2012**, *8*, 2991−2996.
(117) Kang, R. H.; Yao, J. N.; Chen, H. *J. Chem. Theory Comput.* **2013**, *9*, 1872−1879.
(118) Pratt, L. M.; Voit, S.; Mai, B. K.; Nguyen, B. H. *J. Phys. Chem. A* **2010**, *114*, 5005−5015.
(119) Pratt, L. M.; Voit, S.; Okeke, F. N.; Kambe, N. *J. Phys. Chem. A* **2011**, *115*, 2281−2290.
(120) Sun, Y. Y.; Chen, H. *J. Chem. Theory Comput.* **2013**, *9*, 4735−4743.
(121) Sun, Y. H.; Chen, H. *J. Chem. Theory Comput.* **2014**, *10*, 579−588.
(122) Kang, R. H.; Chen, H.; Shaik, S.; Yao, J. N. *J. Chem. Theory Comput.* **2011**, *7*, 4002−4011.
(123) Ehm, C.; Budzelaar, P. H. M.; Busico, V. *J. Organomet. Chem.* **2015**, *775*, 39−49.
(124) Varganov, S. A.; Olson, R. M.; Gordon, M. S.; Mills, G.; Metiu, H. *J. Chem. Phys.* **2004**, *120*, 5169−5175.
(125) Ciancaleoni, G.; Rampino, S.; Zuccaccia, D.; Tarantelli, F.; Belanzoni, P.; Belpassi, L. *J. Chem. Theory Comput.* **2014**, *10*, 1021−1034.
(126) Sun, Y. Y.; Hu, L. R.; Chen, H. *J. Chem. Theory Comput.* **2015**, *11*, 1428−1438.
(127) Zhao, Y.; Truhlar, D. G. *J. Chem. Theory Comput.* **2009**, *5*, 324−333.
(128) Piacenza, M.; Hyla-Kryspin, I.; Grimme, S. *J. Comput. Chem.* **2007**, *28*, 2275−2285.
(129) Kesharwani, M. K.; Martin, J. M. L. *Theor. Chem. Acc.* **2014**, *133*, 1452.
(130) Kazaryan, A.; Baerends, E. J. *J. Comput. Chem.* **2013**, *34*, 870−878.
(131) Weymuth, T.; Couzijn, E. P. A.; Chen, P.; Reiher, M. *J. Chem. Theory Comput.* **2014**, *10*, 3092−3103.
(132) Seth, M.; Ziegler, T.; Steinmetz, M.; Grimme, S. *J. Chem. Theory Comput.* **2013**, *9*, 2286−2299.
(133) Faza, O. N.; Rodríguez, R. Á.; López, C. S. *Theor. Chem. Acc.* **2011**, *128*, 647−661.

DOI: 10.1021/acs.jctc.5b00373
J. Chem. Theory Comput. 2015, 11, 4601−4614

(134) Fang, H. C.; Li, Z. H.; Fan, K. N. *Phys. Chem. Chem. Phys.* **2011**, *13*, 13358−13369.
(135) Purvis, G. D.; Bartlett, R. J. *J. Chem. Phys.* **1982**, *76*, 1910−1918.
(136) Watts, J. D.; Gauss, J.; Bartlett, R. J. *J. Chem. Phys.* **1993**, *98*, 8718−8733.
(137) Frisch, M. J.; Trucks, G. W.; Schlegel, H. B.; Scuseria, G. E.; Robb, M. A.; Cheeseman, J. R.; Scalmani, G.; Barone, V.; Mennucci, B.; Petersson, G. A.; Nakatsuji, H.; Caricato, M.; Li, X.; Hratchian, H. P.; Izmaylov, A. F.; Bloino, J.; Zheng, G.; Sonnenberg, J. L.; Hada, M.; Ehara, M.; Toyota, K.; Fukuda, R.; Hasegawa, J.; Ishida, M.; Nakajima, T.; Honda, Y.; Kitao, O.; Nakai, H.; Vreven, T.; Montgomery, J. A., Jr.; Peralta, J. E.; Ogliaro, F.; Bearpark, M.; Heyd, J. J.; Brothers, E.; Kudin, K. N.; Staroverov, V. N.; Kobayashi, R.; Normand, J.; Raghavachari, K.; Rendell, A.; Burant, J. C.; Iyengar, S. S.; Tomasi, J.; Cossi, M.; Rega, N.; Millam, J. M.; Klene, M.; Knox, J. E.; Cross, J. B.; Bakken, V.; Adamo, C.; Jaramillo, J.; Gomperts, R.; Stratmann, R. E.; Yazyev, O.; Austin, A. J.; Cammi, R.; Pomelli, C.; Ochterski, J. W.; Martin, R. L.; Morokuma, K.; Zakrzewski, V. G.; Voth, G. A.; Salvador, P.; Dannenberg, J. J.; Dapprich, S.; Daniels, A. D.; Farkas, O.; Foresman, J. B.; Ortiz, J. V.; Cioslowski, J.; Fox, D. J. *Gaussian 09*, revision C.01; Gaussian, Inc.: Wallingford, CT, 2009.
(138) Waller, M. P.; Braun, H.; Hojdis, N.; Bühl, M. *J. Chem. Theory Comput.* **2007**, *3*, 2234−2242.
(139) Kim, J.; Ihee, H.; Lee, Y. S. *J. Chem. Phys.* **2010**, *133*, 144309.
(140) Bühl, M.; Reimann, C.; Pantazis, D. A.; Bredow, T.; Neese, F. *J. Chem. Theory Comput.* **2008**, *4*, 1449−1459.
(141) Zhao, S.; Li, Z. H.; Wang, W. N.; Liu, Z. P.; Fan, K. N.; Xie, Y.; Schaefer, H. F., III. *J. Chem. Phys.* **2006**, *124*, 184102.
(142) Pierloot, K.; Vancoillie, S. *J. Chem. Phys.* **2008**, *128*, 034104.
(143) Dunning, T. H. *J. Chem. Phys.* **1989**, *90*, 1007−1023.
(144) Dunning, T. H.; Peterson, K. A.; Wilson, A. K. *J. Chem. Phys.* **2001**, *114*, 9244−9253.
(145) Peterson, K. A.; Figgen, D.; Dolg, M.; Stoll, H. *J. Chem. Phys.* **2007**, *126*, 124101.
(146) Figgen, D.; Peterson, K. A.; Dolg, M.; Stoll, H. *J. Chem. Phys.* **2009**, *130*, 164108.
(147) Becke, A. D. *Phys. Rev. A.* **1988**, *38*, 3098−3100.
(148) Perdew, J. P. *Phys. Rev. B.* **1986**, *33*, 8822−8824.
(149) Lee, C. T.; Yang, W. T.; Parr, R. G. *Phys. Rev. B.* **1988**, *37*, 785−789.
(150) Handy, N. C.; Cohen, A. J. *Mol. Phys.* **2001**, *99*, 403−412.
(151) Zhao, Y.; Truhlar, D. G. *J. Chem. Phys.* **2006**, *125*, 194101.
(152) Tao, J.; Perdew, J. P.; Staroverov, V. N.; Scuseria, G. E. *Phys. Rev. Lett.* **2003**, *91*, 146401.
(153) Perdew, J. P.; Burke, K.; Ernzerhof, M. *Phys. Rev. Lett.* **1996**, *77*, 3865−3868.
(154) Ernzerhof, M.; Scuseria, G. E. *J. Chem. Phys.* **1999**, *110*, 5029−5036.
(155) Adamo, C.; Barone, V. *J. Chem. Phys.* **1999**, *110*, 6158−6170.
(156) Becke, A. D. *J. Chem. Phys.* **1993**, *98*, 5648−5652.
(157) Zhao, Y.; Truhlar, D. G. *Theor. Chem. Acc.* **2008**, *120*, 215−241.
(158) Boese, A. D.; Martin, J. M. L. *J. Chem. Phys.* **2004**, *121*, 3405−3416.
(159) Chai, J. D.; Head-Gordon, M. *J. Chem. Phys.* **2008**, *128*, 084106.
(160) Yanai, T.; Tew, D. P.; Handy, N. C. *Chem. Phys. Lett.* **2004**, *393*, 51−57.
(161) Vydrov, O. A.; Heyd, J.; Krukau, A. V.; Scuseria, G. E. *J. Chem. Phys.* **2006**, *125*, 074106.
(162) Vydrov, O. A.; Scuseria, G. E. *J. Chem. Phys.* **2006**, *125*, 234109.
(163) Karton, A.; Tarnopolsky, A.; Lamere, J. F.; Schatz, G. C.; Martin, J. M. L. *J. Phys. Chem. A* **2008**, *112*, 12868−12886.
(164) Grimme, S. *J. Chem. Phys.* **2006**, *124*, 034108.
(165) Chen, K. J.; Zhang, G. L.; Chen, H.; Yao, J. N.; Danovich, D.; Shaik, S. *J. Chem. Theory Comput.* **2012**, *8*, 1641−1645.
(166) Chen, H.; Lai, W. Z.; Yao, J. N.; Shaik, S. *J. Chem. Theory Comput.* **2011**, *7*, 3049−3053.
(167) Chen, H.; Cho, K.-B.; Lai, W. Z.; Nam, W.; Shaik, S. *J. Chem. Theory Comput.* **2012**, *8*, 915−926.
(168) Grimme, S.; Antony, J.; Ehrlich, S.; Krieg, H. *J. Chem. Phys.* **2010**, *132*, 154104.
(169) Goerigk, L.; Grimme, S. *J. Chem. Theory Comput.* **2011**, *7*, 291−309.
(170) Chai, J. D.; Head-Gordon, M. *Phys. Chem. Chem. Phys.* **2008**, *10*, 6615−6620.
(171) Werner, H.-J.; Knowles, P. J.; Lindh, R.; Manby, F. R.; Schütz, M.; Celani, P.; Korona, T.; Mitrushenkov, A.; Rauhut, G.; Adler, T. B.; Amos, R. D.; Bernhardsson, A.; Berning, A.; Cooper, D. L.; Deegan, M. J. O.; Dobbyn, A. J.; Eckert, F.; Goll, E.; Hampel, C.; Hetzer, G.; Hrenar, T.; Knizia, G.; Köppl, C.; Liu, Y.; Lloyd, A. W.; Mata, R. A.; May, A. J.; McNicholas, S. J.; Meyer, W.; Mura, M. E.; Nicklass, A.; Palmieri, P.; Pflüger, K.; Pitzer, R.; Reiher, M.; Schumann, U.; Stoll, H.; Stone, A. J.; Tarroni, R.; Thorsteinsson, T.; Wang, M.; Wolf, A. *MOLPRO*, version 2010.1, a package of ab initio programs. See http://www.molpro.net.
(172) Knizia, G.; Adler, T. B.; Werner, H. J. *J. Chem. Phys.* **2009**, *130*, 054104.
(173) Adler, T. B.; Knizia, G.; Werner, H. J. *J. Chem. Phys.* **2007**, *127*, 221106.
(174) Schwenke, D. W. *J. Chem. Phys.* **2005**, *122*, 014107.
(175) Hill, J. G.; Peterson, K. A.; Knizia, G.; Werner, H. J. *J. Chem. Phys.* **2009**, *131*, 194105.
(176) Knizia, G.; Werner, H. J. *J. Chem. Phys.* **2008**, *128*, 154103.
(177) Weigend, F. *J. Comput. Chem.* **2008**, *29*, 167−175.
(178) The def2-AQZVPP/JKFIT basis set contains one even-tempered diffuse function for each primitive set of Weigend's def2-QZVPP/JKFIT in ref 177 and was taken from the Molpro basis set library.
(179) Weigend, F. *Phys. Chem. Chem. Phys.* **2002**, *4*, 4285−4291.
(180) The aug-cc-pVTZ/JKFIT basis set contains one even-tempered diffuse function for each primitive set of Weigend's cc-pVTZ/JKFIT in ref 179 and was taken from the Molpro basis set library.
(181) Hill, J. G.; Platts, J. A. *J. Chem. Theory Comput.* **2009**, *5*, 500−505.
(182) Hill, J. G. *J. Chem. Phys.* **2011**, *135*, 044105.
(183) Weigend, F.; Kohn, A.; Hattig, C. *J. Chem. Phys.* **2002**, *116*, 3175−3183.
(184) Hill, J. G.; Peterson, K. A. *J. Chem. Theory Comput.* **2012**, *8*, 518−526.
(185) Martin, J. M. L. *Chem. Phys. Lett.* **1996**, *259*, 669−678.
(186) Feller, D.; Peterson, K. A.; Hill, J. G. *J. Chem. Phys.* **2011**, *135*, 044102.
(187) Hill, J. G. *J. Comput. Chem.* **2013**, *34*, 2168−2177.
(188) Lim, B. S.; Sung, K. M.; Holm, R. H. *J. Am. Chem. Soc.* **2000**, *122*, 7410−7411.
(189) Note that consistent with all the other data discussed herein, C−H activation energy was calculated as the difference between the transition state energy and the reactant complex energy.

DOI: 10.1021/acs.jctc.5b00373
J. Chem. Theory Comput. 2015, 11, 4601−4614